Assessment of flamelet-based models for liquid ammonia combustion in a temporally evolving mixing layer

Jiangkuan Xing*, Zhenhua An, Abhishek Lakshman Pillai, Ryoichi Kurose

Department of Mechanical Engineering and Science, Kyoto University, Kyoto, daigaku-Katsura, Nishikyo-ku, Kyoto 615–8540, Japan

Abstract: Liquid ammonia needs to co-fired with small-molecular fuels, such as methane, to achieve stable combustion, and liquid ammonia will undergo flash boiling under relatively low ambient pressure. Those features multiple fuel streams and strong local heat loss, posing challenges to the flamelet modelling of liquid ammonia combustion. To this end, this study aims to evaluate the flamelet-based models for liquid ammonia combustion. Firstly, a three-dimensional Carrier-Phase Direct Numerical Simulation (CP-DNS) was conducted to explore the combustion characteristics of a liquid ammonia/methane co-fired flame in a temporally evolving mixing layer. The results revealed multiple stages in the liquid ammonia/methane co-fired flame, namely, the mixing stage, methane-dominated stage, and main reaction stage. Subsequently, flamelet-based models were developed with the complex fuel streams, strong local heat loss, and combustion modes considered, and their performances were assessed through a priori analyses. (137 words)

Keywords: Liquid ammonia flame, DNS, FPV, FGM, Hybrid model

1. Introduction

To promote reduced carbon emissions and sustainable energy, the use of ammonia as an alternative, carbon-free fuel and hydrogen carrier has gained increasing interest. Application of liquid ammonia can reduce the costs on storage and pre-evaporations equipment [1]. To date, there have been limited studies on the spray and combustion of liquid ammonia [1-5], yet numerical simulations of it remain limited. The low boiling temperature of liquid ammonia makes it undergo flash boiling under atmospheric condition, resulting a fast phase change and strong local heat loss. Liquid ammonia flame usually need to be stabilized with the help of pilot flame of small-molecular fuels, such as methane [1], which leads to multiple fuel streams. Flamelet approach has been approved to be efficient in many previous studies [6-8]. The suitability of flamelet-based combustion models for liquid ammonia combustion and how to consider the multiple fuel streams and strong heat loss in liquid ammonia flame are still open questions.

To this end, the present study aims to assess the performance of flamelet-based models for liquid ammonia combustion modelling. First, a three dimensional Carrier-Phase Direct Numerical Simulation (CP-DNS) of co-fired liquid ammonia/methane flame in a temporally evolving mixing layer was conducted to explore the combustion characteristics of liquid ammonia flame, and also used as a reference for the evaluation of the following flamelet models. Second, three flamelet models, including the flamelet progress variable (FPV), flamelet generated manifold (FGM), and a hybrid model that combined the FPV and FGM through flame index, are developed and examined in *a priori* analysis with the CP-DNS solutions as benchmarks.

2. CP-DNS coupled with detailed chemistry

In the CP-DNS, the gas-phase governing equations, including the continuous, momentum, species, and enthalpy, are solved without any averaging and filtering. For the dispersed phase, the conservation equations, including the position, velocity, and temperature are solved under the Lagrangian framework. The phase change process of ammonia droplets is described using a combined model that we developed and validated in our previous study [5]. The two-way coupling method is used to describe the interactions between gas and droplets. The details of all conservation equations are not introduced here for brevity and the interested readers can refer to our previous studies [3,5, 9,10].

3. Flamelet-based models for liquid ammonia flame

Flamelet approach tabulates the combustion chemistry using several control variables [11]. For diffusion and premixed flames, FPV [12] and FGM [13] models are used, respectively. In the current work, three models are developed, named the E-FPV, E-FGM, and E-Hybrid models. Compared with traditional FPV and FGM models, we introduced two extra parameters, X (fuel ratios) and He (total enthalpy), to consider the complex fuel streams and heat loss. Specifically, the thermochemical properties can be tabulated as

$$\varphi = \varphi(Z, X, PV, He_{norm}) \quad (1)$$

$$Z = Z_{NH3} + Z_{CH4} \quad (2)$$

$$X = Z_{CH4}/Z \quad (3)$$

where Z_{CH4}, Z_{NH3}, and Z is the methane, ammonia and total mixture fractions. Respectively. Those mixture fractions are also solved in the CP-DNS. PV is the progress variable, which is defined as the sum of the mass fractions of H2O, CO2, and H2, which is directly obtained from the DNS results in the a priori study. He_{norm} is the normalized total enthalpy, and X is used to distinguish the local fuel sources as our previous study [9].

To construct the flamelet tables, one-dimensional counter-flow diffusion flames and freely-propagating flames under different X values and initial temperatures are calculated. X ranges from 0 to 1 with an interval of 0.1. When X value equals to 0 or 1, the local fuel would be pure ammonia or methane, respectively. For E-FPV tables, the fuel temperature T_f is set to be equal to the oxidizer temperature T_{ox} to represent the interphase heat transfers, and ranges from 250 to 2100 K. Note that this 250 K is considered here to consider the strong heat loss by flash boiling. For E-FGM tables, equivalence ratios of 1D freely-propagating premixed flame range from 0.5 to 2.0 with an interval of 0.1. Different initial temperatures from 250 to 700 K are considered to represent the heat loss effect. In addition, pure oxidizer and fuel solutions are also used to make sure the completeness of the E-FGM tables in the mixture fraction space.

In the E-Hybrid model, the flame index which is defined as [14] to access the local combustion mode,

$$FI = \frac{1}{2}\left(1 + \frac{\nabla Y_F \cdot \nabla Y_{O_2}}{|\nabla Y_F||\nabla Y_{O_2}|}\right) \quad (4)$$

where Y_F and Y_{O2} are mass fractions of fuels (CH_4 and NH_3) and oxidizer, respectively. The final prediction of the hybrid model is obtained by $\varphi_{E-Hybrid} = \varphi_{E-FGM} + (1 - FI)\varphi_{E-FPV}$.

Figure 1 shows the flamelet solution in the mixture fraction space of the 1D one-dimensional counter-flow diffusion flames and freely-propagating flames under different X values and temperatures. Note that for counter-flow diffusion flame, the flamelet profiles are shown in the mixture fraction space. While for the freely-propagating flames, each flamelet only has one mixture fraction value, thus they are shown in the progress variable space. It is found with the fuel/oxidizer temperature increases, the general temperature increases, which indicates that heat loss are important in the flame behavior. With the increasing of ammonia fraction in the fuel stream, the flame temperature gradually decreases, which is because of the relatively lower heat value of ammonia. As for premixed flamelets, as methane fraction in the fuel stream increases, the maximum progress variable increase, and this is the same as that when equivalence ratio increases.

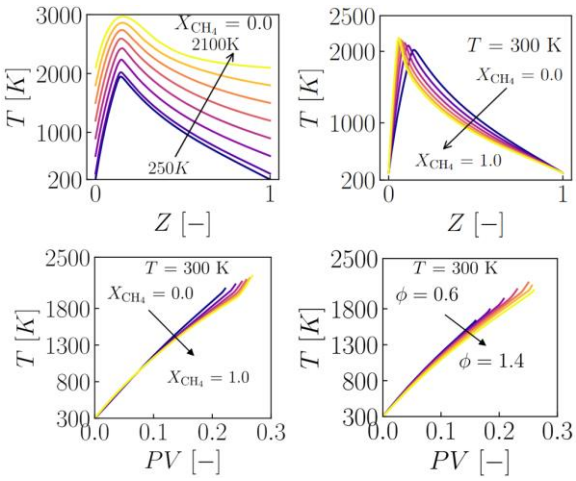

Figure 1 Top: 1D flamelet profiles of temperature of counter-flames under different T and X_{CH4} values. Left: X_{CH4} = 0.0, T = 250 - 2100 K, right: T_o = 300 K, X_{CH4} = 0.0-1.0. Bottom: 1D flamelet profiles of temperature of freely propagating flames under different X_{CH4} and equivalence ratios. Left: T=300 K, X_{CH4} =0.0-1.0, ∅=1.0, right: X_{CH4} =0.4, T=300 K, ∅ = 0.6-1.3.

4. Computational setup

Figure 2 shows the computational domain of the temporally evolving liquid ammonia flame with dimension of Lx × Ly × Lz = 24×24×12 mm^3 and a uniform grid of 480×480×240. The mesh resolution is sufficient to resolve the flame thickness and Kolmogorov scale according to our previous studies [5]. Liquid ammonia (L_{NH3}) droplets and premixed mixture of methane and air are injected into the upper half of the computational domain with velocity of 21 m/s, carrier gas preheating temperature of 500 K, and droplets temperature of 279 K. All the droplets are randomly distributed in the upper domain. The heat fraction of ammonia is 0.7, the overall equivalence ratio is 1.0, and the pressure is 0.25 MPa which are referred to the experimental configurations [1]. For the lower part of the domain, the properties of co-flow are determined by calculated results of NH_3/CH_4/air flames under the same condition. The velocity of hot-burnt mixture is 1 m/s. The periodic boundary conditions are applied to left and right sides.

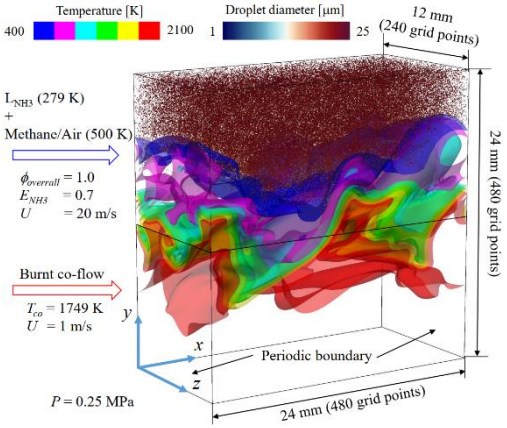

Figure 2 Computational domain and boundary conditions for temporally evolving liquid ammonia flame. The ammonia droplets and iso-surfaces of temperature are depicted.

5. Results and discussion

Figure 3 shows the temporal evolution of liquid ammonia flame from initial condition to burnt state. The regions represent temperature fields and distributions of ammonia droplets. It can be found that the liquid ammonia droplet evaporates rapidly after 7 ms. The temperature of carrier gas increases after 5 ms.

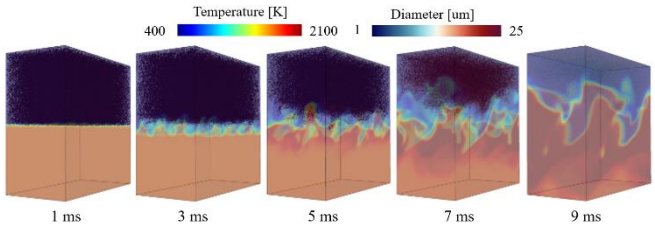

Figure 3 Temporal evolution of temperature fields and distributions of ammonia droplets for liquid ammonia flame from 1 - 9 ms.

The fuel source contains flashed ammonia and methane. The phase change process of liquid ammonia will absorb the heat from surrounding gas, resulting a strong local heat loss. The ignition delay time of methane is much smaller than that of ammonia. Methane will be consumed first, and then ammonia is consumed. Therefore, the combustion process of L_{NH3}/CH_4/air flames can be divided into three stages, as shown in Fig. 4. In the first stage (S1), the temperature keeps decreasing, which indicate an inert evaporation and mixing stage. In the second stage (S2), the temperature increase, liquid ammonia keeps evaporating, and the main contribution of HRR comes from reacting of methane. In the third stage (S3), the ammonia mass fraction decreases, ammonia keeps consumed, and in this stage, liquid ammonia totally evaporates. Clearly state that we will discuss three time instant to do the a priori analyses.

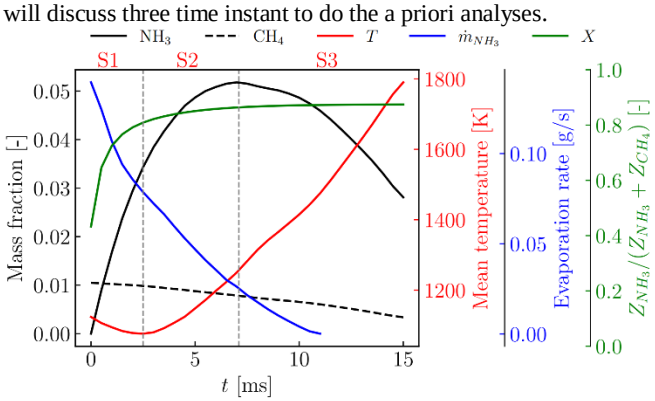

Figure 4 Temporal evolution of volume averaged mass fractions of NH_3 and CH_4, mean temperature of carrier gas, evaporation rate of ammonia droplets, and fraction of Z_{NH3} in Z_{NH3} + Z_{CH4}. S1, S2, and S3 represent mixing, methane-dominated, and fully reacting stages, respectively.

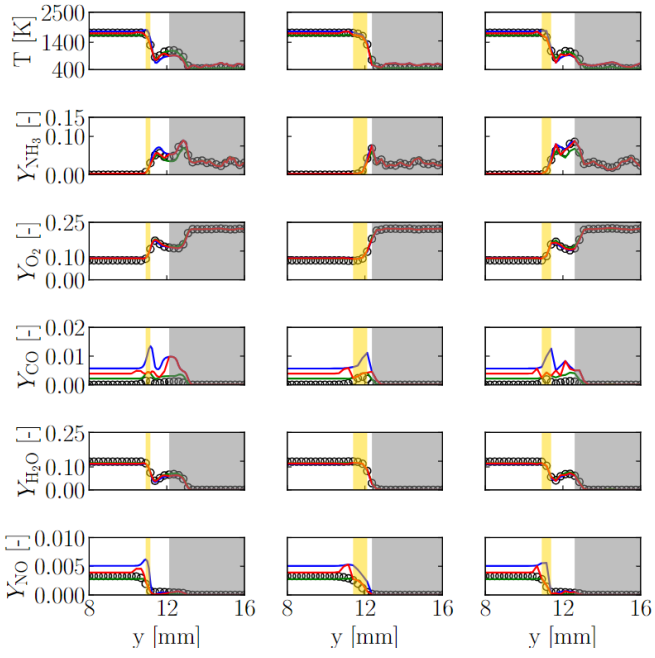

Figure 5 Comparisons between DNS results and priori profiles of E-FGM (green line), E-FPV (blue line), and E-Hybrid models (red line) at t = 1 ms (S1) for different spatial locations. Left: x/Lx = 1/4, middle: x/Lx = 1/2, right: x/Lx = 3/4. The gray and yellow shadows represent the non-premixed and premixed combustion mode, respectively.

Figure 5 shows the Comparisons between DNS results and priori profiles of E-FGM (green line), E-FPV (blue line), and E-Hybrid models (red line) at t = 1 ms, which represents the inert mixing stage. In this stage, heat is absorbed by ammonia droplets, while the flame has not been ignited. As for the temperature field, it can be found that E-FPV overestimates the value, but E-FGM underestimates it in the co-flow side. The hybrid model accurately predicted the temperature value here. However, in the fresh side, the E-FGM predict well. For CO mass fraction, these models are unable to accurately well reproduce the DNS solutions, which may be caused by the definition of progress variable. E-FGM accurately predicted the value of NO, which could be attributed to the fact that the lower stream features a hot burnt mixture of coal volatiles and ammonia.

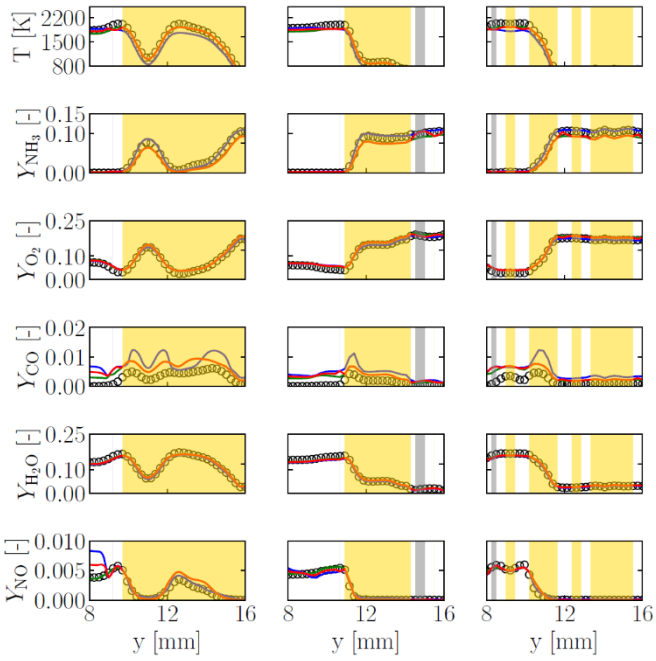

Figure 6 Comparisons between DNS results and priori profiles of E-FGM (green line), E-FPV (blue line), and E-Hybrid models (red line) at t = 5 ms (S2) for different spatial locations. Left: x/Lx = 1/4, middle: x/Lx = 1/2, right: x/Lx = 3/4. The gray and yellow shadows represent the non-premixed and premixed combustion mode, respectively.

Figures 6 and 7 shows the comparisons of the DNS solutions and E-FGM/E-FPV/E-Hybrid models for stages S2 and S3, respectively. Because of quick evaporation and mixing process, the proportion of non-premixed modes is very small when t = 5 ms and 7 ms. Most of the region features premixed combustion mode. The superiority of the FGM and Hybrid models retains, especially for the prediction of intermediate species, such as CO and NO mass fractions. For the gas temperature prediction, E-FGM and E-Hybrid models can also give better predictions. In the S3, the mixing proceeds more thoroughly, the premixed mode dominates the whole region. Therefore, the results of FGM and hybrid models are nearly the same (see green and red line). The superiority of the FGM and Hybrid models retains, especially for NO predictions.

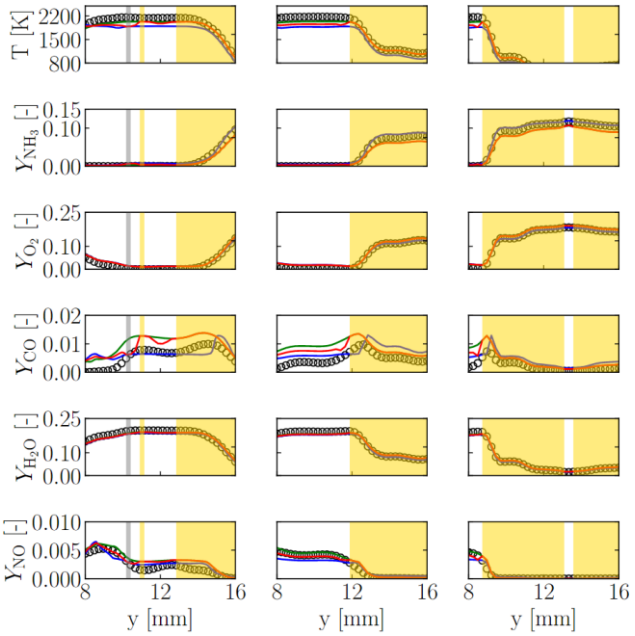

Figure 7 Comparisons between DNS results and priori profiles of E-FGM (green line), E-FPV (blue line), and E-Hybrid models (red line) at t = 9 ms (S3) for different spatial locations. Left: x/Lx = 1/4, middle: x/Lx = 1/2, right: x/Lx = 3/4. The gray and yellow shadows represent the non-premixed and premixed combustion mode, respectively.

6. Conclusion

This study assessed the flamelet-based models in liquid ammonia combustion in a temporally evolving mixing layer. Firstly, a 3D DNS was conducted, and three reacting stages were identified: mixing stage, methane-dominated stage, and fully reacting stage. Then, E-FPV, E-FGM, and E-Hybrid models were developed and evaluated through the *a priori* study. Through the comparison of predictions of the E-FPV, E-FGM, and E-Hybrid models with DNS solutions as benchmarks, it can be seen that for the simulation of liquid ammonia combustion, the premixed flamelet constructed E-FGM has a better performance than that of E-FPV. This can be attributed to the fast flash boiling and sufficient mixing of the flashed ammonia vapor. In the future study, E-FGM and E-Hybrid models can be used for numerical simulation of liquid ammonia combustion.

Acknowledgement

This work was partially supported by MEXT as “Program for Promoting Researches on the Supercomputer Fugaku” (Development of the Smart design system on the supercomputer “Fugaku” in the era of Society 5.0) (JPMXP1020210316). This research used the computational resources of supercomputer Fugaku provided by the RIKEN Center for Computational Science (Project ID: hp220180, hp230193, hp220141).

Reference

[1] Okafor, E. C., Kurata, O., Yamashita, H., et al., ***Applications in Energy and Combustion Science***, 2021, 7: 100038.
[2] Li, S., Li, T., Wang, N., et al., ***Fuel***, 2022, 324: 124683.
[3] An, Z., Xing. J., Pillai, A., Kurose, R., ***Fuel***, 2023, accepted.
[4] Okafor, E. C., Yamashita, H., Hayakwa, A., et al., ***Fuel***, 2021, 287: 119433.
[5] An, Z., Xing. J., Kurose, R., ***Fuel***, 2023, 345, 128229.
[6] Baba, Y., Kurose, R., ***Journal of Fluid Mechanics***, 2008, 612:

45-79.
[7] Xing, J. Luo, K., Chen, Y., et al., ***Proceedings of the Combustion Institute***, 2021, 38: 5347-5354.
[8] Hu, Y., Kurose, R., ***Combustion and Flame***, 2018, 188: 227-242.
[9] Xing, J., Luo, K., Kurose, R., et al. ***Proceedings of the Combustion Institute***, 2023, 39(3): 3227-3237.
[10] Xing, J., Luo, K., Wang, H., ***Energy & Fuels***, 2023, 34(3): 3816-3827.
[11] Pitsch, H., ***Annual Review of Fluid Mechanics***, 2006, 38: 453-482.
[12] Pierce, C. D., Moin, P., ***Journal of Fluid Mechanics***, 2004, 504: 73-97.
[13] Van Oijen, J. A., Donini, A., Bastiaans, R. J. M., et al., ***Progress in Energy and Combustion Science***, 2016, 57: 30-74.
[14] Yamashita, H., Shimada, M., Takeno, T., ***Proceedings of the Combustion Institute***, 1996, 26: 27-34.